Flux parameterization in the representative elementary watershed approach: Application to a natural basin

P. Reggiani
Foundation Delft Hydraulics, Delft, Netherlands

T. H. M. Rientjes[1]
International Institute for Geo-Information Science and Earth Observation, Enschede, Netherlands

Received 29 September 2004; accepted 13 January 2005; published 23 April 2005.

[1] An integrated hydrological modeling approach based on the discretization of a watershed into spatial units called representative elementary watersheds (REWs) has been introduced in earlier publications. Global balance laws were formulated at the spatial scale of a REW by integrating the point-scale conservation equations over particular control volumes. The choice of the control volumes is subject to the specific flow behavior to be described and is dependent on the hydrological characteristics of the spatial regions. These include the unsaturated subsurface flow, groundwater flow, and overland and channel flow. The REW-scale balance laws constitute generally valid governing equations for environmental flows encountered in hydrological systems and are applicable, in contrast to point-scale equations, independently from the chosen spatial and temporal scale of representation. This paper presents a first application of the REW approach to a complex hydrological system and shows how a theory that has so far only been used for synthetic cases is applicable to real-world situations. In this context the most challenging research effort remains the formulation of appropriate closure schemes for mass and momentum (and energy) fluxes at the REW scale. It is recognized that the schemes proposed for the closure of the fluxes in this paper are subject to limitations but are sufficient to expose the philosophy and the essential working principles. The advantages of the particular spatial discretization and the current limitations of the closure schemes are highlighted. In this context it is pointed out which way future research should go to consolidate the REW approach as a more general and scale-independent modeling philosophy for hydrological systems.

Citation: Reggiani, P., and T. H. M. Rientjes (2005), Flux parameterization in the representative elementary watershed approach: Application to a natural basin, *Water Resour. Res.*, *41*, W04013, doi:10.1029/2004WR003693.

1. Introduction

[2] The demands by policymakers, implementers and stakeholders with respect to the prognostic capabilities of hydrological models become increasingly sophisticated. Experts are asked to predict hydrological variables, such as water table depth, soil saturation, saturated surface area fractions, flow velocity as well as hydrological fluxes like bare soil evaporation, plant transpiration and water table recharge in a spatially distributed fashion and at a level of accuracy not demanded previously. These demands are primarily driven by two motives: First, it is widely recognized that decisions on land use practices, deployment of infrastructure, exploitation of natural resources or change of climate can irreversibly perturb local and large-scale equilibria of hydrological systems and subsequently alter runoff behavior, water yield and quality, with potentially severe socioeconomic implications for stakeholders, economic actors and the population living within or downstream of the watershed boundaries. Second, there is a common belief, which is however not shared by several experts that the recently experienced leap in availability and affordability of radar, spaceborne, and airborne high-resolution data sets will lead to significant progress in the representation of hydrological systems through models, thus bringing a "sufficiently accurate" description within reach.

[3] In response to these requests from end users, hydrologists traditionally propose two kind of modeling approaches with their respective strong points and limitations: (1) physically based and (2) conceptual catchment models.

[4] Physically based models consist of formulations in terms of physical laws expressed in the form of deterministic conservation equations for mass, momentum, and energy at the point scale. The equations are solved numerically by discretizing the hydrological system into smaller entities on a square or a polygonal mesh. *Freeze and Harlan* [1969] proposed a general blueprint for building distributed

[1] Also at Section of Water Resources, Delft University of Technology, Delft, Netherlands.

0043-1397/05/2004WR003693$09.00

hydrological models that rests on partial differential equations (PDEs) governing flow through soils (Richards' equation, Darcy's law), overland flow (kinematic wave equation) and open channel flow (Saint-Venant equations). This blueprint forms the theoretical basis for a series of distributed approaches to follow throughout the literature. The first and most complete is the SHE by *Abbott et al.* [1986a, 1986b], followed by other approaches such as IHDM described by *Calver and Wood* [1995], HILLFLOW by *Bronstert* [1999], or InHM employed by *Van der Kwaak and Loague* [2001].

[5] There has been considerable discussion regarding the pros and cons of this type of models by *Beven* [1989], *Grayson et al.* [1992], *Refsgaard and Storm* [1996], *Beven* [1996], and *O'Connell and Todini* [1996], with the conclusion drawn by some authors that physically based distributed hydrological modeling has clear limitations. While the aim is to apply conservation equations for mass and momentum at the point scale to obtain a deterministic continuum representation of the system, its implementation has not led to the prediction skill achieved by continuum models in other fields such as oceanography, limnology or meteorology. The reasons here fore are manifold. Foremost the intrinsic weakness of a point-scale continuum approach in a hydrological context is due to the fact that PDEs describe flow at the spatial scale of a soil core sample or REV. The use of such a continuum description rarely yields results with a quality level that would justify employing these tools routinely for hydrological predictions, including the expensive acquisition of input information at the required spatial resolution. This shortcoming is mainly attributable to the extreme degree of heterogeneity of the substratum, the unclear definition of the model domain, the lack of knowledge on the boundary conditions and the questionable success in describing the (often non-Darcian) flow behavior through point-scale equations, a problem that is intrinsic to hydrological systems (but is not encountered to that extent in hydrodynamic problems). Moreover does the computational demand of this kind of models preclude their use for large-scale modeling applications like those envisaged for impact studies of climate and land use change on water yields at large, say regional or national scales.

[6] As an alternative to physically based distributed models, conceptual catchment models are often used as robust prognostic tools. Because of the simplicity of their structure, mostly a series of interconnected reservoirs, they are invaluable instruments for operational water management (e.g., reservoir operation, flood forecasting). In this group of models we list the lumped Stanford Watershed Model described by *Crawford and Linsley* [1966], the semi-distributed TOPMODEL [*Beven and Kirkby*, 1979], the USGS model PRMS [*Leavesley et al.*, 1983] based on hydrologically representative units (HRUs), the HBV model by *Bergström* [1995], and the large-scale catchment model LASCAM of *Viney and Sivapalan* [1999]. In most cases the description of the reservoir's behavior is kept simple and their response controlled by parameterizations that are rarely interpretable in terms of physical principles and quantities such as gravity, piezometric heads or hydraulic conductivities. To obtain a satisfying reproduction of lumped hydrological responses the parameters are tuned manually, or automatically by means of optimization algorithms [e.g., *Duan et al.*, 1993]. However, once environmental forcing conditions (e.g., switching from wet to dry conditions) or catchment characteristics (e.g., land cover pattern) change, the parameters usually need to be recalibrated. Because of conceptualization and simplification of the described processes the models adapt with difficulty to external change and in particular hydrological extremes, which amongst others are the motive for carrying out long-term and large-scale hydrological studies in the first place. Lumped tools moreover preclude to account explicitly for hydrological state variables such as water table position, groundwater-river interaction and lateral groundwater redistribution that play a pivotal role in the feedback between the lower atmosphere and the groundwater-soil-vegetation continuum. An explicit description of these processes requires the use of the spatial physically based and/or process-oriented tools mentioned earlier.

[7] In view of these facts, *Reggiani et al.* [1998, 1999, 2000] introduced the REW concept, which rests on global balance laws for mass, momentum and energy formulated for representative hydrological control volumes. This approach is now implemented and constitutes, as stated by *Beven* [2002], an alternative blueprint for describing a hydrological system. Starting from the topography a catchment is broken down into a series of irregularly shaped modeling volumes, the REWs. The very definition of the REW allows its recognition at various spatial scales. It yields a general building block that is independent of the scale of discretization chosen by the modeler. It also does not constrain the discretization to a square grid, but allows for an irregular mesh of elements that reflect the natural footprint of the landscape.

[8] The physical model is based on megascale (for definition, see *Gray et al.* [1993]) or REW-scale conservation laws for mass, momentum and energy. Thanks to the way the equations are formulated, it differs from lumped conceptual or distributed physically based models. The essential difference lies in the integrated flux-based formulation, in which physical laws and quantities such as piezometric heads and forces are preserved (in contrast to lumped conceptual models). The REW-scale mass fluxes represent area-integrated water exchanges between the various internal zones. The REW-scale momentum exchange terms are the pressure forces integrated over the control volume boundaries that drive horizontal flow between REWs. However, the interpretation of these quantities is not straightforward and their definition acquires to some extend conceptual character, in particular as heterogeneity and small-scale variability within the REW are accounted for only in an averaged fashion. In contrast to the *Freeze and Harlan* [1969] blueprint, variations within a chosen spatial region are averaged, and transformed into interactions across the volume boundaries. A small-scale application of a flux-based formulation is given by *Duffy* [1996]. He gives an example of a flux-based control volume formulation in hydrology, where the closure problem for mass fluxes across the boundaries of a unsaturated-saturated zone hillslope system is exposed as a hydrological challenge per se. This work nicely shows that the difficulties of implementing such a formulation lie essentially in the correct parameterization of the relevant hydrological fluxes.

[9] The definition of the REW and the spatially independent scaling procedure of conservation laws from the microscale to the megascale (or REW scale) are generally valid and should draw the attention of the hydrologist naturally toward improving and refining closure schemes, rather than on contemplating small-scale process descriptions or opting for higher spatial resolutions, a common trajectory in the frame of the *Freeze and Harlan* [1969] philosophy. An additional feature of the REW approach is the incorporated averaging of the balance equations in time. This fact encourages the use of the approach for studying hydrological problems that extend over a wide range of temporal scales. For example water yield and change impact studies might require simulation of hydrological systems over several decades, and therefore not require knowledge of dynamic variable fluctuations over temporal scales in the order of weeks or less. On the other hand these become important when investigating the response of a system to single forcing events, as for operational use in flood or water quality prediction.

[10] In the following sections the concepts underlying the REW approach are presented. By means of a simulation exercise for a study site it is shown how REWs can be routinely extracted from a digital elevation map and how a system can be modeled in its entirety, while shortcomings and limitations are critically evaluated. The exposition is structured in 4 consecutive sections. Section 2 briefly shows the integration principle for the balance laws from the microscale to the REW scale, section 3 reports the parameterization of the equations, section 4 describes the application for the Geer study case, while section 5 summarizes the conclusions and further research needs.

2. REW-Scale Balance Laws

2.1. Choice of the Control Volumes

[11] *Reggiani et al.* [1998, 1999] partitioned a watershed into a series of discrete spatial units called representative elementary watersheds (REWs). REWs are defined by topographic analysis and constitute a set of the interconnected volumes that are organized around the binary tree structure of the stream channel network, as shown in Figure 1. REW boundaries coincide with the topographic divides that delineate subcatchments linked to the drainage network. The REW is a three-dimensional spatial entity delimited externally by a prismatic mantle that follows the shape of the subcatchment contour. A schematic representation of an ensemble of 3 REWs is depicted in Figure 2. On top the REW is delimited by the atmosphere and below by an impermeable layer or a chosen limit depth. The volume occupied by a REW contains different flow zones. The flows within the zones extend over characteristic temporal scales and typically encompass unsaturated and saturated groundwater flow (subsurface zones) and Manning-type overland and channel flow (land surface zones). If necessary additional zones such as a perched zone or a subsurface storm flow zone can be added following the same principles. The REW volumes have been called representative because their repetitive structure (ensemble of typical flow zones) can be recognized at increasingly smaller spatial scales by zooming in from the entire catchment down to arbitrary smaller subbasins. These can in principle become arbitrary small, as long as they contribute to a specific network link

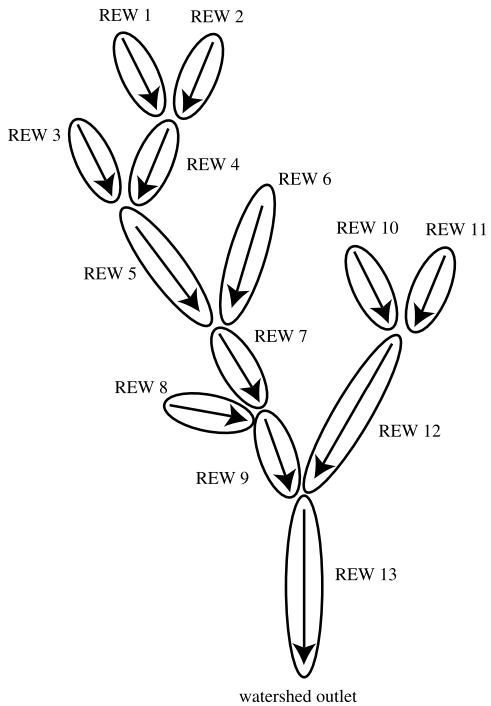

Figure 1. Aggregation of 13 REWs following the binary tree structure of the channel network.

and are delimited by their own identifiable topographic boundaries. This definition guides the REW extraction procedure from a digital elevation map. As shown closer in section 4.2, a drainage network analysis is carried out first. The REWs are subsequently identified by choosing a given Strahler order as threshold and identifying the respective 3-D drainage regions contributing to the individual network links as modeling elements or REWs.

2.2. Changing Scale

[12] In the context of the REW approach, balance laws for mass, momentum, and energy are mapped from the microscale or point scale to the megascale (or REW scale) by integration in space. Additional integration over a characteristic timescale has also been proposed. Balance laws are derived for each phase (solid, air, water) and each zone of a REW. The resulting conservation equations constitute ordinary differential equations (ODEs) that have the following general form for each phase and each flow zone of a REW:

$$\frac{d\psi}{dt} = \sum_i e_i^{\psi} + R + G \tag{1}$$

where ψ represents a generic property such as mass, momentum or energy, e_i^{ψ} is a generic watershed-scale exchange term for ψ, R is an external supply term for ψ (e.g., a body force or radiation energy supply) and G is its internal production. The exchange terms account for the transfer of ψ among phases, zones and REWs. We emphasize that all ODEs of type (1) constitute global balance laws. These equations represent the respective balance of a property through REW-averaged dynamic variables and fluxes and are referred to as megascopic or megascale equations of *Gray et al.* [1993]. The exchange or

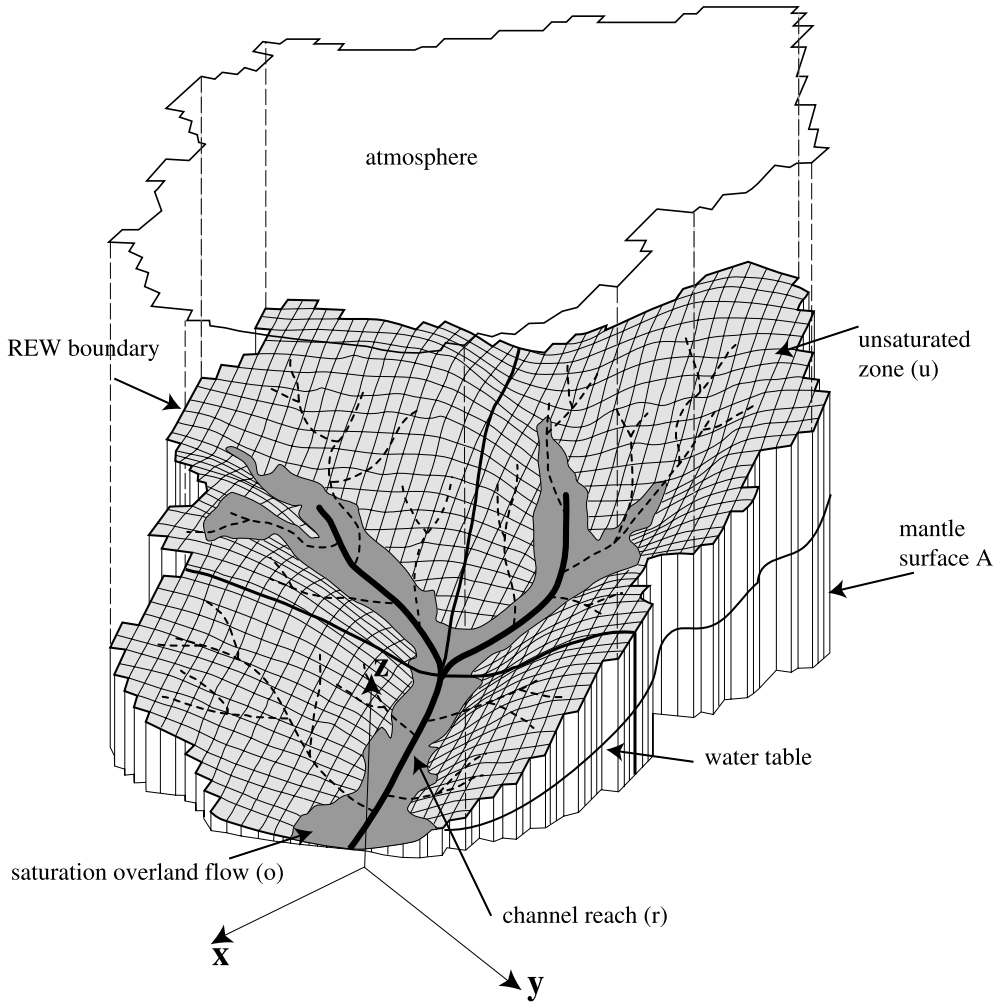

Figure 2. Three-dimensional view of an ensemble of three REWs, including a portion of atmosphere.

flux terms e_i^{ψ} result from the integration and constitute unknowns of the problem. As such, they require appropriate closure parameterizations. An attempt to obtain these within a single and physically consistent procedure was made by *Reggiani et al.* [1999] by using the second law of thermodynamics as a constraint. This procedure has led to linearized parameterizations of the fluxes. In this paper preliminary ad hoc closure schemes are employed following hydrological experience. This is considered one of the main contributions of the present work with respect to previous theoretical papers. The closure however remains an issue that should be the focus for further research on developing and testing systematically new and improved schemes.

2.3. REW-Scale Governing Equations

[13] The aim of this work is an integrated description of a hydrological system underlain by a regional aquifer that reaches beyond its topographic boundaries. The water table of each REW is recharged by precipitation that filtrates from the surface through an unsaturated zone of consistent depth.

[14] The aquifer feeds the base flow in the drainage network through exchange from the aquifer into the river across the channel bed surface. To capture these processes in terms of the governing physical principles, REW-scale conservation laws for mass and momentum are stated for the water phase in four flow zones within a REW. The required balance equations have already been derived in earlier publications. They are summarized in Tables 1 (the mass balance equations) and 2 (the momentum equations). We note that the momentum balance equations require projection along the two horizontal axes $\mathbf{e_x}$, $\mathbf{e_y}$ and the vertical axis $\mathbf{e_z}$ of a global reference system, while for the saturated overland flow and the channel flow zone the balance equations are projected along resultant flow directions $\mathbf{n^o}$ and $\mathbf{n^r}$ directed along the surface and the channel axis, respectively. Some of the force terms are assumed negligible and will drop out as shown in section 3.3. The superscripts u, s, o, and r refer to the unsaturated zone, the saturated zone, the saturated overland flow zone and the river reach. We note that the equations have been divided by the constant mass density ρ. In section 3.2 we show how the mass

Table 1. Mass Balance Equations

Zone	Mass Balance Equations
Unsaturated zone	$\Sigma\ \epsilon \frac{d}{dt}\,(s^u y^u \omega^u) = e^{us} + e^{u\ top} + e^u_{wg}$
Saturated zone	$\Sigma\ \epsilon \frac{d}{dt}\,(y^s \omega^s) = \sum_{i=1,N} e^{sm\ i} + e^{su} + e^{so} + e^{sr}$
Channel reach	$l^r \frac{d}{dt}\,(m^r) = e^{ro} + e^{rs} + e^{r\ in} + e^{r\ out}$
Overland flow	$\Sigma\ \frac{d}{dt}\,(y^o \omega^o) = e^{os} + e^{or} + e^{o\ top}$

Table 2. Momentum Balance Equations

Zone	Momentum Balance Equations
Unsaturated zone	$\Sigma \epsilon s^u y^u \omega^u \frac{d}{dt} \mathbf{v}^u - \Sigma \mathbf{g} \epsilon s^u y^u \omega^u = \sum_{i=1,N} \mathbf{T}^{um\ i} + \mathbf{T}^{us} + \mathbf{T}^{u\ top} + \mathbf{T}^u_{wg} + \mathbf{T}^u_{wm}$
Saturated zone	$\Sigma \epsilon y^s \omega^s \frac{d}{dt} \mathbf{v}^s - \Sigma \mathbf{g} \epsilon y^s \omega^s = \sum_{i=1,N} \mathbf{T}^{sm\ i} + \mathbf{T}^{s\ bot} + \mathbf{T}^{so} + \mathbf{T}^{sr} + \mathbf{T}^{su} + \mathbf{T}^s_{wm}$
Channel reach	$l^r m^r \frac{d}{dt} \mathbf{v}^r = \mathbf{g} m^r l^r + \mathbf{T}^{rs} + \mathbf{T}^{r\ out} + \mathbf{T}^{r\ in}$
Overland flow	$\Sigma \omega^o y^o \frac{d}{dt} \mathbf{v}^o = \Sigma \mathbf{g} \omega^o y^o + \mathbf{T}^{os} + \mathbf{T}^{or}$

fluxes are closed via suitable parameterizations, while in 3.3 we report relevant assumptions on the momentum terms and respective parameterizations.

3. Parameterizations

3.1. Formulation of the Problem

[15] To reduce the mass and momentum balance laws into parameterized differential equations that are tractable for a real-world application, it is necessary to close the expressions for the mass exchanges e^u_{wg}, e^{us}, $e^{u\ top}$, e^{or}, e^{rs}, $e^{r\ in}$, $e^{r\ out}$, e^{os}, $e^{o\ top}$ and e^{sm} in the conservation equations in Table 1. The same is valid for the nonzero momentum exchange terms $\mathbf{T}^{us}$, $\mathbf{T}^{u\ top}$, $\mathbf{T}^u_{wm}$, $\mathbf{T}^{os}$, $\mathbf{T}^s_{wm}$, $\mathbf{T}^{um\ i}$, $\mathbf{T}^{sm\ i}$, $\mathbf{T}^{r\ out}$, $\mathbf{T}^{r\ in}$, $\mathbf{T}^{rs}$ in the projected momentum balance equations in Table 2. In this fashion we obtain mass and momentum equations that contain a series of parameters and quantities that need to be estimated through measurements, heuristically or on theoretical grounds. Before going into detail on the proposed solution it is important to identify the principal aims of what is to be presented next, by putting its potential and limitations clearly into perspective.

3.1.1. Aims

[16] As stated in the introduction the REW approach rests on the idea that mass and momentum (and energy) fluxes need to be closed for respective balance equations formulated at the chosen scale. Here we want to show how this is feasible in practice for a catchment system, by attempting to reproduce some of its most relevant response features within the framework of a flux-based formulation. We are aware that particular approximations shown here need to be improved. However, the scope of this paper is not to seek perfection in megascale flux parameterization, but rather to show a complete and working first-cut closure attempt that should trigger research curiosity in improving these parameterizations following an outlined philosophy.

3.1.2. Potential

[17] The principal strength of the approach is believed to lie in the reliance on generally valid and scale-independent balance equations at the megascale that help bypassing the scale issues inherent to the use of point-scale governing equations, their range of applicability and how to use them for an integrated description of a hydrological system. The integral formulation of megascale equations yields simple scale-independent expressions that are even solvable analytically under certain restrictive assumptions. By adopting a flux-based formulation the focus shifts from representing flow behavior within the system toward describing interaction on its boundaries. The difficulties related to scale-dependent representation of flows encountered in the *Freeze and Harlan* [1969] approach are deferred toward tackling the parameterization of the fluxes. Working with megascale equations requires researching flux closure (and respective parameterization) rather than searching for optimal parameter sets in a continuum representation at high spatial resolution. The ability to represent fluxes correctly will become the benchmark criterion for accepting or rejecting a proposed REW-scale model.

3.1.3. Limitations

[18] We emphasize that the proposed flux closure schemes are preliminary and constitute an extension of the work by *Reggiani et al.* [2000, 2001]. These schemes may lead in some cases to model deficiency that is due to the chosen parameterizations. An improvement of the parameterizations must be considered to enhance model behavior. The actual choice of new closure formulations will remain dependent on the particular hydrological situation. The improvement of the flux parameterization is to be pursued on theoretical and/or observational grounds. For some fluxes reliable measurements at the required spatial scale may sooner or later become available (e.g., scintillometer estimates of evaporation fluxes), other fluxes will always remain difficult to measure (e.g., groundwater fluxes). For the latter flux parameterizations will have to be deduced based on quantitative knowledge on system behavior, such as analytical solutions of vadose zone moisture movement [e.g., *Haverkamp et al.*, 1990], or heuristically, guided by realism and hydrological intuition. The choice of describing a system at the proposed spatial scale might moreover lead to deficiencies attributable to the negligence or to the averaged representation of heterogeneity and small-scale variability within the system. In some hydrological situations it may result less efficient than using continuum representations. These facts have to be explicitly weighted off on a case-by-case basis against possible advantages when opting for this approach. Finally, in view of these observations, a flux-based approach will not be able to overcome limitations already encountered in other model approaches such as the use of effective parameter values or parameter equifinality that remain a common source of criticism for distributed physically based as well as conceptual approaches.

3.2. Parameterization of the Mass Equations

[19] All mass fluxes must satisfy the continuity conditions across both, internal and external boundaries of the REW and its internal flow zones. Such boundaries are for example the water table, the saturated overland flow source areas, the land surface or the channel bed. The mass exchange terms are generally driven by differences in piezometric head $h = p/\rho g + \zeta$, where p is the pressure and ζ the center of mass position of a particular volume or zone, and/or the flow velocities on either side of the boundary. The parameterizations adopted for the mass fluxes are summarized in Table 3. The expressions $e^{u\ top}$, e^{us}, e^{so}, e^u_{wg}, e^{or}, e^r, and $e^{o\ top}$ have been already introduced

Table 3. Parameterized Mass Balance Equations[a]

Denomination	Flux Term Symbol	Parameterized Expression	Length Scale
Infiltration	$e^{u\ top}$	$\min\left[I\omega^u\Sigma, \frac{K_{sat}\,\omega^u\,\Sigma}{\Lambda^u}(h^c - h^u)\right]$	$\Lambda^u = y^u\ s^u$
GW recharge/capillary rise	$e^{us} = -e^{su}$	$\omega^u\ \epsilon\ v^u\|_z\Sigma$	N/A
Lateral flux through mantle segment i	$e^{sm\ i}$	$\frac{2\,C^i}{[K_{sat}]^{-1}+\left[K^i_{sat}\right]^{-1}}\left[\frac{y^{Ci}}{\Lambda^{si}}\right](h^{s\ i} - h^s)$	$\Lambda^{s\ i}$
Exfiltration on seepage face	$e^{so} = -e^{os}$	$\frac{K_{sat}\,\omega^o\,\Sigma}{\cos\,\gamma^o\Lambda^s}(h^o - h^s)$	$\Lambda^s = \sqrt{\Sigma/\pi}$
Evaporation	e^u_{wg}	$e_p\ \omega^u\ s^u\Sigma$	N/A
Evaporation from overland flow	$e^{o\ top}$	$\min[e^{so},\ \omega^o\ e_p\ \Sigma]$	N/A
Lateral inflow to channel	$e^{or} = -e^{ro}$	$2\ l^r\ v^o$	N/A
Inflow channel	$e^{l\ in}$	$m^{l\ in}\ (v^r + v^{l\ in})/2$	N/A
Inflow channel	$e^{r\ in}$	$m^{r\ in}\ (v^r + v^{r\ in})/2$	N/A
Channel outflow	$e^{r\ out}$	$m^r\ (v^r + v^{r\ out})/2$	N/A
Channel-GW exchange	$e^{sr} = -e^{rs}$	$\frac{P^r l^r K^r_{bot}}{\Lambda^r}(h^r - h^s)$	Λ^r

[a]N/A is not applicable.

by *Reggiani et al.* [2000, 2001]. A closer description can be found there and is thus omitted for the sake of brevity. The parameterization of the inter-REW groundwater fluxes across the mantle segments $e^{sm\ i}$ and the groundwater-channel interaction e^{sr} are introduced here for the first time and warrant some more in-depth description. For a parsimonious estimation of $e^{sm\ i}$ we apply a parameter estimation procedure based on the Hardy-Cross method for pipe or resistor networks.

3.2.1. Groundwater Flow Across the REW Mantle Surface

[20] The REW interacts with a number N of neighboring REWs, with which it exchanges mass across the mantle segments, $e^{sm\ i}$. This mass exchange is governed by the difference of hydraulic heads between a given REW and its ith neighbor. We can now express the mass exchange as a difference in total pressure head across the mantle segment:

$$e^{sm\,i} = \alpha^{s\,i}\left(h^{s\,i} - h^s\right) \tag{2}$$

where h^s is the piezometric head and the coefficient $\alpha^{s\,i}$ is defined as follows:

$$\alpha^{s\,i} = \frac{2C^i}{\left[\frac{1}{K_{sat}} + \frac{1}{K^i_{sat}}\right]}\frac{y^{C^i}}{\Lambda^{s\,i}} = \frac{2C^i}{\left[\frac{1}{K_{sat}} + \frac{1}{K^i_{sat}}\right]}\Theta^i \tag{3}$$

The quantity $C^i = \sqrt{\left(C^i_x\right)^2 + \left(C^i_y\right)^2}$ is the resultant straight length of the contour curve of the ith mantle segment (see Figure 3), $2/(1/K_{sat} + 1/K^i_{sat})$ is the harmonic mean of the saturated hydraulic conductivities between the REW and its ith neighbor, and y^{C^i} the aquifer thickness in correspondence of the ith mantle segment centroid. y^{C^i} is approximated by interpolating the REW water table positions y^s in space. $\Lambda^{s\,i}$ is an unknown length scale. The ratio $\Theta^i = y^{C^i}/\Lambda^{s\ i}$ constitutes thus an unknown that needs to be estimated based on the principles of mass continuity and piezometric head conservation between the groundwater zones of connected REWs. For this purposes a resistor network algorithm for water distribution networks has been employed. A detailed description of the algorithm would go beyond the scope of this paper. A brief introduction is thus given hereunder. Equations (2) and (3) are also applied to simulate mass exchanges across the permeable edges of the watershed. This is done by imposing a hydraulic head value at the external boundary. The effective cross sectional flow area for the ith mantle segment, $A^{m\ i}$ is approximated with the product of the contour length with the depth of the aquifer on the mantle segment:

$$A^{m\,i} = C^i\,y^{C^i} \tag{4}$$

3.2.2. Procedure for the Calculation of Θ^i

[21] For the calculation of the ratios Θ^i we propose the use of an equation system based on the Kirchoff laws for

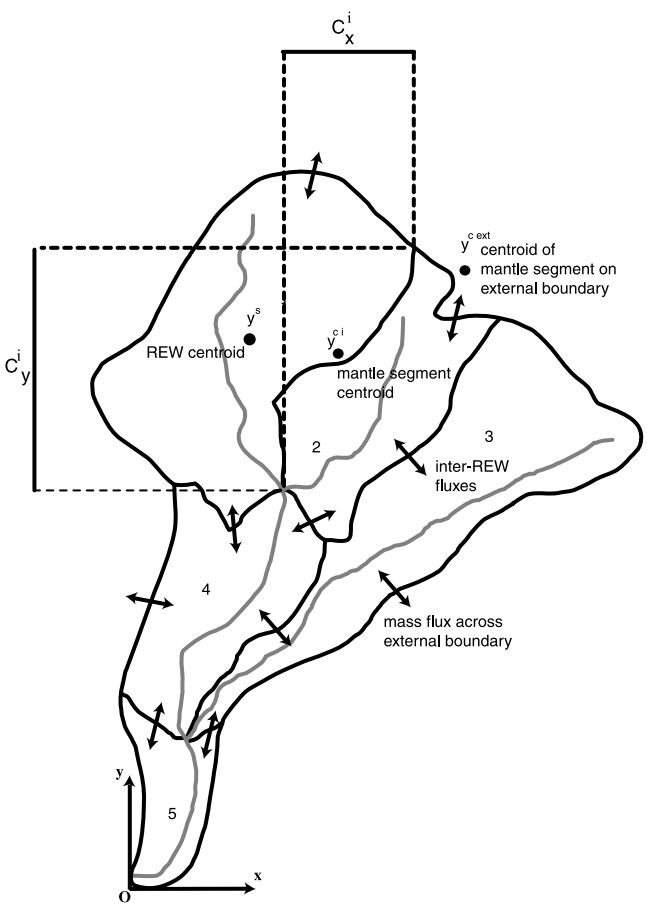

Figure 3. Horizontal projection of a watershed partitioned into five REWs.

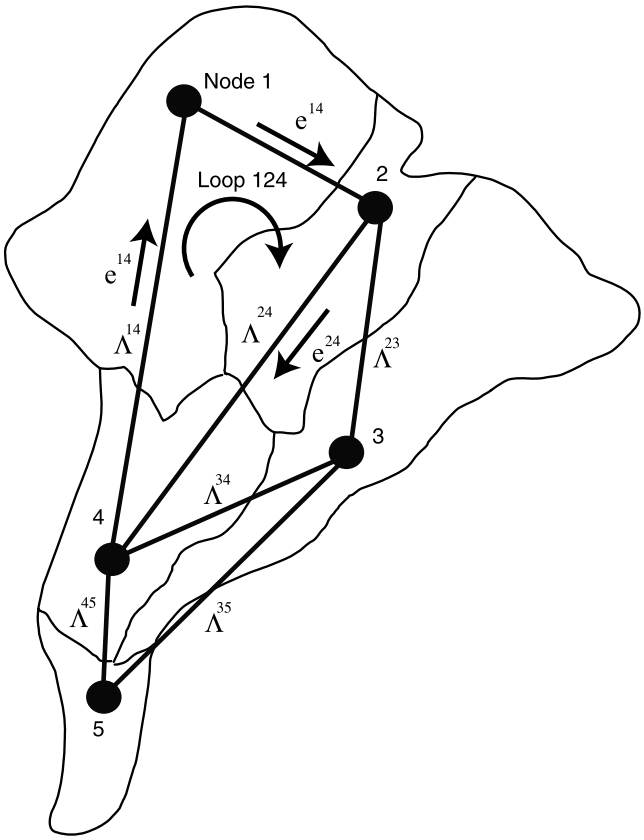

Figure 4. The pipe network for a watershed separated into five REWs.

resistor networks. To pursue this approach, it is assumed that the aquifer is at any time sufficiently close to the steady state. This assumption seems reasonable given the generally slow flow regime in the aquifer for which the time derivatives of the dynamic variables become negligible. As shown in Figure 4, the aquifer underlying the watershed is separated into a finite number of REWs and can be envisaged as a network of pipes of length $\Lambda^{s\,i}$ interconnecting nodes. The quantities $\Lambda^{s\,i}$ constitute the unknown length scales, over which inter-REW pressure heads are dissipated.

[22] By requiring that the sum of head losses along a closed network loop equals zero and that the sum of discharges entering and exiting a network node adds up to zero (equivalent to the mass conservation for the saturated zone of a REW), the problem is reduced to the solution of a nonlinear system. The solution is obtained by successive approximation by applying the Hardy-Cross [see *Cross*, 1936] procedure. At convergence a steady state discharge distribution for the terms (indicated as in Figure 4) is found. Given a known piezometric head distribution at the network nodes (or REW centroids) at a given point in time, unique values for the coefficients can be calculated via (2) and (3). These are then used for the solution of the saturated zone mass balance equation in Table 1 under dynamic (non-steady) conditions.

3.2.3. Groundwater-Channel Flow Interaction

[23] In the present REW formulations it is assumed in extension to the work of *Reggiani et al.* [2000] that the saturated zone interacts with the channel reach and that mass exchange between the two zones is possible. The mass

Table 4. Parameterized Momentum Balance Equations

Zone	Momentum Balance Equations	Parameters
Unsaturated zone	$\Sigma\, g\, \epsilon\, s^u\, y^u\, \omega^u = [-p^u/\rho + 1/2\, g\, y^u]\, \Sigma - R^u\, v_z^u$	$p^u/\rho = h_{bc}\,(s^u)^{1/\lambda}$, Brooks-Corey pressure scaling relationship; $R^u = y^u\, g\, \Sigma/[K_{sat}\,(s^u)^{\eta}]$, flow resistance; Σ, horizontal REW surface area projection; ϵ, porosity; s^u, REW-averaged saturation of the unsaturated zone (from mass balance equation); y^u, average depth of the unsaturated zone (from geometric relationship); $\omega^u = 1 - \omega^o$, unsaturated REW area fraction (geometric relationship)
Saturated zone	$\sum_{i=1,N} [\frac{1}{2}\, g\, y^{C_i}]\, A_\lambda^{m\ i} + [\frac{1}{2}\, g\, y^{C\ ext}]\, A_\lambda^{m\ ext} - R^s\, v_\lambda^s = 0;\ \lambda = x, y$	N, number of neighboring REWs; $A_\lambda^{m\ i} = C_\lambda^i\, y^{C_i}$, vertical surface area projection of the ith mantle segment; $A_\lambda^{m\ ext} = C_\lambda^{ext}\, y^{C\ ext}$, vertical surface area projection of mantle segment on external watershed boundary; $R^s = y^s\, g\, \Sigma/K_{sat}$, flow resistance; y^s, average depth of the saturated zone (from mass balance equation); y^{C_i}, $y^{C\ ext}$, depth of saturated zone in correspondence of mantle segments (calculated via 2-D bicubic spline interpolation of y^s, refer to Figure 3)
Channel reach	$l^r\, m^r\, \frac{d}{dt}\, v^r = g \sin\beta^r\, m^r\, l^r + (m^{in} + m^{out})\, p^r/\rho - M^r\, \lvert v^r\rvert\, v^r$	$p^r = 1/2\, g\, \rho\, y^r$, hydrostatic pressure; $M^r = P^r\, l^r\, g\, (n^r)^2/(m^r/P^r)^{1/3}$, flow resistance; n^r, channel Manning friction factor; m^r, m^{in}, m^{out}, reach-averaged cross section, inlet and outlet sections (from mass balance equation); l^r, y^r, P^r, channel length, depth and wetted perimeter (from geometric relationships)
Overland flow	$\Sigma\, \omega^o\, y^o\, \frac{d}{dt}\, v^o = \Sigma\, \omega^o\, g \sin\beta^o\, y^o - M^o\, \lvert v^o\rvert\, v^o$	$M^o = \Sigma\, \omega^o\, g\, (n^o)^2/(y^o)^{1/3}$, flow resistance; n^o, overland flow Manning friction factor; y^o, overland flow depth (from mass balance equation); ω^o, saturated area fraction (from geometric relationships)

exchange is calculated through a simple expression based on hydraulic head differences between the saturated zone and the river reach:

$$e^{sr} = \alpha^{sr}(h^r - h^s) \tag{5}$$

The linearization coefficient α^{sr} is approximated as:

$$\alpha^{sr} = \frac{P^r l^r K^r_{bot}}{\Lambda^r} \tag{6}$$

where Λ^r is a length scale characterizing the thickness of the channel bed transition zone, K^r_{bot} is the saturated hydraulic conductivity of the transition zone, l^r is the reach length, and P^r the wetted perimeter of the channel reach (see section 3.3.3 and Table 4).

3.3. Parameterization of the Momentum Equations

[24] Next, suitable expressions for the force terms in the momentum equations need to be introduced. To obtain tractable equations we introduce assumptions that are defendable from a physical as well as hydrological point of view and allow us to simplify the equations in Table 2. These assumptions concern the flow directions and the projection of the REW-scale force terms and can in principle be relaxed at any time. The assumptions have been presented by *Reggiani et al.* [2000] and are omitted here in the interest of brevity. Through application of the assumptions, parameterized expressions for the balance equations are obtained. These are summarized in Table 4. The solution of the equations in terms of the velocities v^u_z, v^s_x, v^s_y and v^o requires the specification of additional quantities for each zone to be introduced in the following sections 3.3.1, 3.3.2, and 3.3.4.

3.3.1. Unsaturated Zone

[25] For the hydrodynamic characterization of the unsaturated zone we apply common practice from soil science. We emphasize that the proposed solution is based on point-scale theory and is used here as an expedient and preliminary solution that need to be replaced in the future by more suitable formulations. We refer to the *Brooks and Corey* [1964] formulation to calculate the capillary pressure under unsaturated conditions. The pressure head $h = p/(\rho g)$ is related to the water content θ via a soil characteristic shape parameter λ and the pressure scaling parameter h_{bc}. The hydraulic conductivity under unsaturated conditions can be related to the saturated hydraulic conductivity K_{sat} and the shape parameter η. The degree of saturation $s^u = \theta^u/\epsilon$ in the unsaturated zone is a REW-averaged value calculated from the mass balance. From s^u average values for water pressure and capillary pressure are estimated. We are aware that in principle, even if the equations hold for smaller, uniform regions within the unsaturated zone, they may not hold at the REW scale. A dependence of the REW-scale capillary pressure on the mean saturation s^u is however to be expected. To account for the lumping effect of small-scale heterogeneity a dependence on other average properties may also be sought. A plausible relationship for the REW-scale pressure head for example is

$$h = h(\theta^u, y^u) \tag{7}$$

At this stage we do however not have sufficient experimental information to define such a relationship and therefore continue based on this preliminary model. The unsaturated zone thickness y^u decreases with increasing depth of the saturated zone as the saturated and the unsaturated volumes compete with each other within the REW subsurface zone. This relation is expressed mathematically via a geometric relationship $y^u = y^u(y^s)$ given by *Reggiani et al.* [2000].

3.3.2. Saturated Zone

[26] To reproduce the hydrologic response of the study basin it is necessary to include the dynamics of the saturation overland flow source areas ω^s. Through a geometric relationship $\omega^s = \omega^s(y^s)$ the area fractions are assumed to grow linearly as a function of the REW-averaged saturated zone depth y^s. If y^s increases above the average river bed elevation within the REW, the source areas expand linearly with y^s. Once the water table reaches the average surface elevation the REW becomes saturated, i.e., $\omega^s = 1$.

[27] The saturated zone thickness at the mantle segment centroids, y^{Ci} (see Figure 3), are estimated by performing a spatial bicubic spline interpolation between the average water table values y^s at the REW centroids. The saturated zone thickness $y^{C\ ext}$ on the mantle segments that overlap with external watershed boundaries are imposed as known boundary conditions. A constant value for the saturated conductivity K_{sat} is assigned to the entire REW saturated zone.

3.3.3. Channel Reach

[28] The solution of the channel flow equations requires knowledge of the channel depth y^r and of the wetted perimeter P^r. These geometric properties can be expressed in terms of the dependent variables m^r and v^r calculated from the balance equations. They are obtained by combining the at-a-station and downstream hydraulic geometry relationships of *Leopold and Maddock* [1953]. The empirical relationships allow us to express the velocity, the top width and the flow depth for a reach as power laws of the discharge. Strictly speaking, they are valid under steady state conditions but are in fact applied to a nonsteady situation. These relationships have been derived by *Snell and Sivapalan* [1995] and were tested on a real-world river system by *Naden et al.* [1999]. The top width w^r, the flow depth y^r and the velocity v^r for any given reach in time (at a station) or along the network at a given point in time (downstream) are expressed as power laws of the discharge $Q^r = m^r v^r$ in the following form:

$$w^r = a(Q^r)^b \tag{8}$$

$$y^r = c(Q^r)^d \tag{9}$$

$$v^r = q(Q^r)^f \tag{10}$$

[29] The scaling coefficients a, c and q are functions of position and thus can in principle vary from reach to reach while the exponents b, d and f are independent of space. The at-a-station wetted perimeter P^r can be approximated by applying these concepts and carrying out a line integration over the channel depth. Details of the derivations are given by *Snell and Sivapalan* [1995] and are omitted here.

3.3.4. Overland Flow

[30] The overland flow equations are solved by making use of the geometric relationship $\omega^o = \omega^o(y^s)$. The solution is dependent on the choice of the Manning roughness parameter

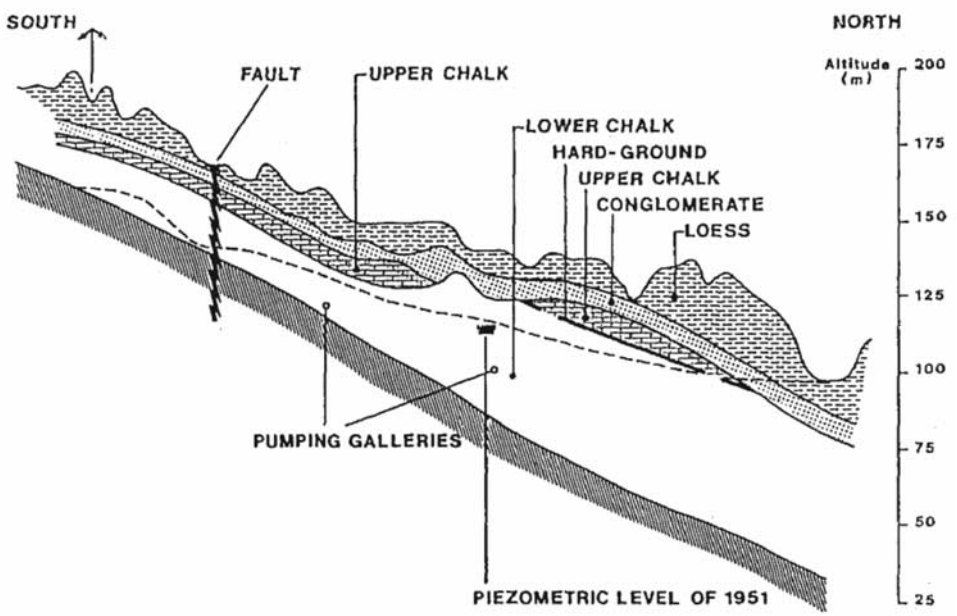

Figure 5. Geological transect of the Geer basin showing the inclined impermeable substratum. Reprinted from *Dassargues et al.* [1988] with permission from Elsevier.

that can vary between REWs. Suitable parameter values can be obtained from the SCS classification [*Soil Conservation Service*, 1972] for various soil and land use types.

4. Application

4.1. Study Site Description

[31] The numerical model is tested on the 494 km^2 basin of the river Geer in Belgium, a tributary of the river Meuse. The catchment area shows strong anthropogenic influence and is characterized by agricultural activities and the presence of numerous smaller urban centers. The study site is crossed by a road network, including the freeway from Antwerp to Luik (Liège) and a major railway link. The river Geer dewaters the basin toward the Belgian-Dutch border. The Geer basin is underlain by the Hesbaye aquifer that is part of a regional groundwater system extending beyond the catchment boundaries. In the river Geer a base flow at a rate of about 1.8 m^3/s is sustained uniformly throughout the year through seepage outflow from the aquifer. The maximum observed peak discharge during the simulation period is of 9 m^3/s. The aquifer consists of cretaceous chalks [see, e.g., *Dassargues and Monjoie*, 1993] with a thickness varying from few meters in the south to about 100 m in the northeast and is confined at the bottom by a layer of smectite that can be considered impermeable. The smectite substratum is inclined from south to the north following a gradient between 1% to 1.5%. A geological transect of the basin is shown in Figure 5.

[32] The vadose zone can reach a thickness of up to 40 m consisting of several layers of chalk stone with measured conductivities in the order of 1–100 m/d [from *Dassargues et al.*, 1988]. The aquifer has a water divide following the surface ridges in the southern part of the basin toward the Meuse valley. From a modeling perspective this boundary can be considered impermeable and is best represented by a no-flux boundary condition. Along the northern edge geological surveys demonstrate that groundwater is discharged across the topographic watershed boundary. This boundary needs to be represented as permeable by allowing for a nonzero groundwater leakage. On the western edge of the basin no-flux boundary conditions apply. *Dassargues et al.* [1988] have modeled the complex aquifer system with a 2760-node Finite Element mesh and spatially varied conductivities for the various mesh layers. A detailed description of the system can be found in the cited publication. Geological surveys [*Brouyère et al.*, 2004] have led to the following estimation of the water balance partitioning for the period from 1975 to 1999:

$$P = ETR + Q_{river} + Q_{out} + Q_{bound} \tag{11}$$

The various quantities have been expressed in millimeters as follows:

$$810\,\text{mm} = 508\,\text{mm} + 145\,\text{mm} + 69\,\text{mm} + 88\,\text{mm} \tag{12}$$

The first two terms on the right-hand side represent the annual evaporation and the volume evacuated through the channel network. The last two terms constitute annual losses for the groundwater system: the extraction through pumping wells and drainage galleries, Q_{out}, and the portion of rainfall lost through leakage across the catchment boundary Q_{bound}. The abstracted water from the Geer basin serves the water supply of the city of Liège and has been exploited in this way since the nineteenth century. For the present application we ignore the presence of pumping wells and drainage galleries and add the corresponding abstracted quantities to the leakage along the northern watershed boundary, thus preserving the overall water balance. The remaining information needed for the simulations are obtained from

Table 5. Model Parameter Values

Parameter	Symbol	Value	Observation
Saturated hydraulic conductivity	K_{sat}	$5e-4$ m/s	constant for entire catchment
Channel bed transition zone thickness	Λ^r	1 m	constant for entire catchment
Hydraulic conductivity channel bed transition zone	K_r	$1e-6$ m/s	constant for entire catchment
Brooks-Corey pressure scaling parameter	h_{bc}	0.25 m	constant for entire catchment
Brooks-Corey pressure shape parameter	λ	0.3	constant for entire catchment
Conductivity shape parameter	η	8.33	constant for entire catchment
Soil porosity	ϵ	0.3	constant for entire catchment
Manning coefficient channel	n^r	0.035	constant for entire catchment
Manning coefficient overland flow	n^o	0.085	constant for entire catchment
Depth scaling exponent	c	0.40	at a station
Width scaling exponent	a	0.33	at a station
Velocity scaling exponent	q	0.34	at a station
Depth scaling exponent	c	0.40	downstream
Width scaling exponent	a	0.5	downstream
Velocity scaling exponent	q	0.1	downstream
Depth scaling coefficient	b	0.23	downstream
Width scaling coefficient	d	7.09	downstream
Velocity scaling coefficient	f	0.61	downstream
Discharge area scaling coefficient	Θ	$2e-6$	see *Snell and Sivapalan* [1995]
Discharge area scaling exponent	Ψ	0.8	see *Snell and Sivapalan* [1995]

field observations and are complemented by assumed values for the pressure scaling parameter and exponents in the Brooks-Corey relationship or the roughness for the channel network and the overland flow areas. The chosen values are listed in Table 5. All soil textural and structural parameters as well as the Manning coefficients are considered homogeneous and uniform in space.

4.2. Model Setup

[33] For the analysis of the catchment topography we use the software TARDEM [*Tarboton*, 1997]. The channel network is extracted by performing a flow accumulation analysis for a 30 × 30 m resolution digital elevation model (DEM). TARDEM flags the DEM pixels belonging to the different drainage areas contributing to the individual network links. Once the network and the subbasins are identified, 3-D REW volumes are extracted. This operation entails the calculation of the REW mantle surface areas, effective slopes and aspects. For this scope the module REWANALYSIS has been developed. REWANALYSIS identifies neighboring REWs and respective lateral connectivities based on nearest neighbor analysis for individual pixels. The contour curves separating two neighboring subbasins are calculated, including their projections onto the

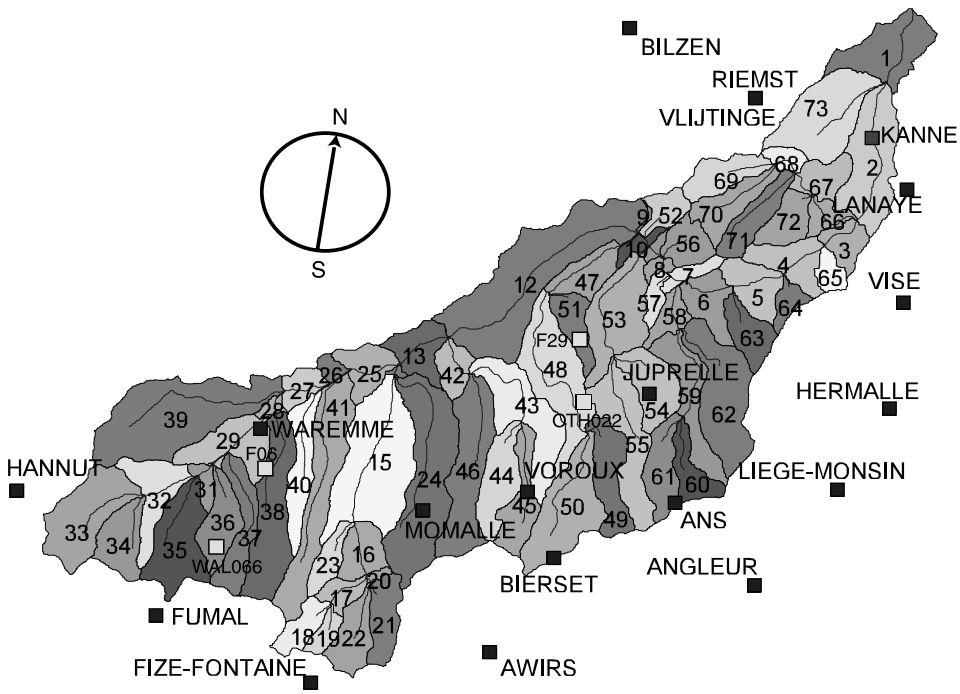

Figure 6. The Geer basin as discretized into 73 REWs, showing the locations of the rain gauges, the piezometer wells, and the Kanne stream gauging station. See color version of this figure in the HTML.

Table 6. Gauging Station Network

Station Name	UTM Easting	UTM Northing	Recording Frequency	Station Type
Hannut Gare	200843	151141	daily	precipitation
Fumal	207468	145183	daily	precipitation
Awris	223842	144089	daily	precipitation
Waremme	212474	154078	daily	precipitation
Bierset	226460	147928	daily	climatic station
Momalle	220220	150190	daily	precipitation
Voroux Goreux	225188	151070	daily	precipitation
Ans	232236	150550	daily	precipitation
Angleur (Bressoux)	236033	146623	daily	precipitation
Lige Monsin	240005	151172	daily	precipitation
Hermalle	242470	155046	daily	precipitation
Vlijtingen	237676	166057	daily	precipitation
Vise (P.C.)	243146	160096	daily	precipitation
Bilzen	230082	173199	daily	precipitation
Lanaye	243304	165507	daily	precipitation
Juprelle	231055	155785	daily	precipitation
Fize Fontaine	243146	160096	daily	precipitation
Kanne (Be-Nl border)	2418101	168289	hourly	discharge

x and y axes of the coordinate system. These curves are defined by the edgy line marking the separation curve between two pixels belonging to two separate but adjacent drainage areas or subbasins (flagged by the TARDEM algorithm). This makes it possible to establish lateral connectivities between REWs and the definition of the groundwater network topology (see section 3.2.2) in an automated fashion. For the proposed application the Geer basin is analyzed by choosing the Strahler order 2 as threshold value, yielding 73 REWs of different size (see Figure 6). A larger number of REWs would have been obtained by opting for the order 1 and higher subbasins.

[34] After assigning the parameter values listed in Table 5 and the required flux/no-flux boundary conditions, appropriate initial conditions need to be imposed. These require a minimum base flow in the channel network, an initial water content for the unsaturated zone, and initial values of the water table position. The latter one is obtained by interpolating piezometric levels from a piezometer monitoring network via 2-D cubic spline functions to average water levels at the REW centroids. The bed rock elevations forming the lower aquifer boundary are assigned following a slightly inclined plane by exploiting geological survey data and using spatial interpolation.

[35] For the meteorological forcing of the model daily measurements of precipitation and potential evaporation (estimated from temperature, wind speed and solar radiation through the Penman-Monteith formula) are mapped from the coordinate points of the gauging stations (for station locations, see squares in Figure 6 and Table 6) through Kriging to the geometrical centroids of the REWs. The computed discharges are compared with hourly values recorded at the gauging station Kanne on the Dutch-Belgian border.

4.3. Simulation Results

[36] For the simulations a 10 year period (1987–1997) is selected. The parameterized ordinary differential equations in Tables 1 and 3 are solved with the aid of an adaptive step-size Runge-Kutta solver based on the *Cash and Karp* [1990] method implemented by *Press et al.* [1994]. The model is run for a duration of 6 years prior to the test period to eliminate the effect of the initial conditions and obtain optimal starting conditions with dynamic model states (internal soil moisture states, water table positions, saturated area extensions) that are at equilibrium with the forcing. The simulation results are obtained without calibration (in the present case limited to parameter optimization, not input correction), based exclusively on parameter values from the literature in order to make model efficiencies as well as its current and general deficiencies more transparent. The computed results are compared directly with measured data. An improvement of model efficiency can be achieved by applying parameter optimization [e.g., *Duan et al.*, 1993] and successive data assimilation via particle tracking or bootstrap filtering [*Doucet et al.*, 2001]. This is matter of ongoing investigations. However, for the present exposure targeted at showing the principles of REW flux parameterization and model implementation uncalibrated results are presented.

[37] Figures 7a and 7b show a comparison between the observed and calculated discharges at the basin outlet (Kanne gauging station in Figure 6). In general the base flow is captured reasonably well by the model over the entire simulation period, with some dips during particular periods that are attributable to a too rapid contraction of the saturated areas. The peak discharges are systematically underestimated. We observe however that the largest aberration between measured and simulated data in correspondence of the first peak at time 4000 hours is evidently due to a discharge measurement error and is not reproduced by the model because the precipitation over the rainfall station network does not show any high values at that point in time (in all 17 stations used). Other simulated and measured discharge peaks correspond with precipitation peaks. Table 7 summarizes three types of error estimations for the entire 2-year simulation period and the year 1996 and 1997 respectively. We observe that the error is in all three cases lower for the year 1997 because of the reason just mentioned.

[38] The Nash-Sutcliffe coefficient results particularly low, in contrast to the mean error, because it emphasizes peak underestimation more than deviations of modeled base flow, which reflects the average annual behavior. The reason for the underestimation of the peaks lies in the intrinsic model deficiencies in representing the mechanisms that contribute to rapid response of the subsurface system. To improve the

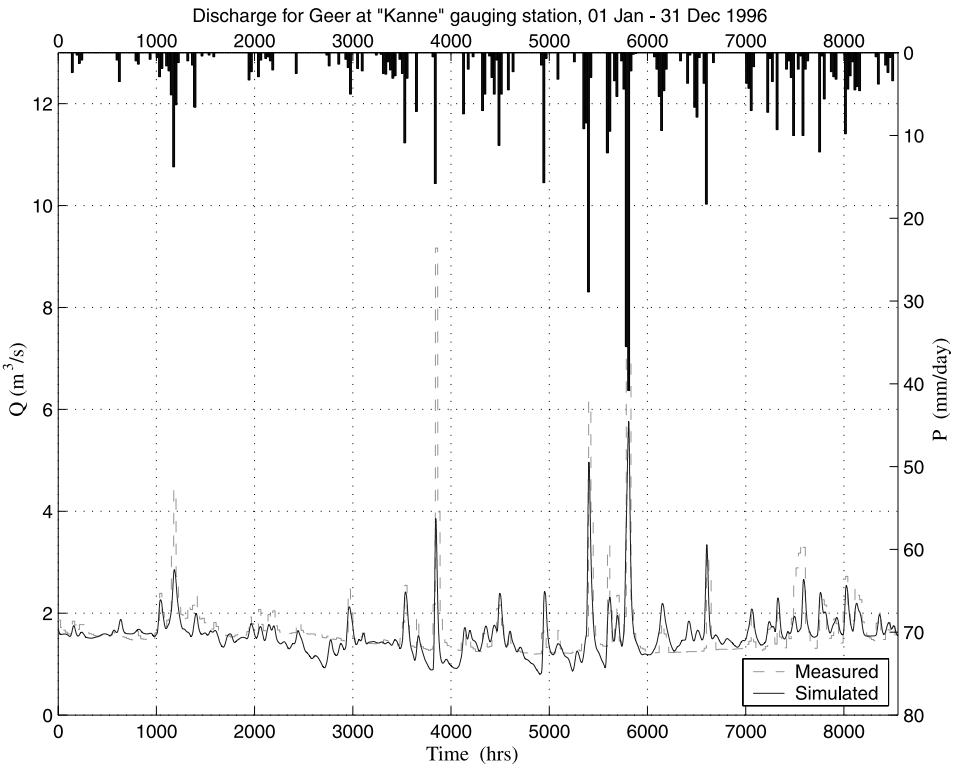

Figure 7a. Measured and simulated hydrograph at Kanne from 1 January 1996 until 31 December 1996.

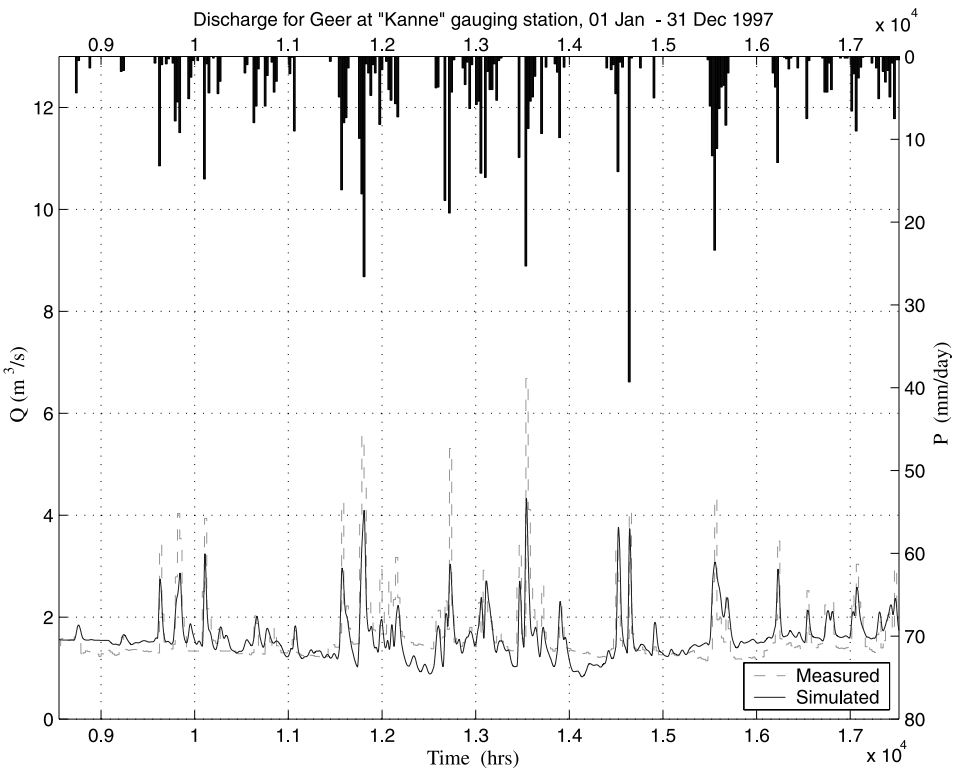

Figure 7b. Measured and simulated hydrograph at Kanne from 1 January 1997 until 31 December 1997.

Table 7. Error Analysis for Outflow at Kanne

Simulation Period	Mean Error	RMSE	Nash-Sutcliffe
1996–1997	0.0791	0.4801	0.3346
1996	0.1090	0.2561	0.3146
1997	0.0492	0.2229	0.3585

model behavior, tests with alternative relationships $\omega(y^s)$ are to be explored. Direct runoff from the saturated areas is not the only mechanism giving raise to quick runoff in the study site. Localized fast groundwater fluctuations and subsurface storm flow in high-permeability layers have not yet been modeled and need to be considered explicitly by including an additional subsurface zone or perched system. This is matter of ongoing research. Effects of urbanization and related infiltration excess flow from sealed areas may also play a nonnegligible role in peak flow generation.

[39] Next we present some principal features of the hydrological fluxes and the internal state variables. To allow a concise representation of the results we decided to plot the various hydrological fluxes and state variables in terms of their mean annual values for the ensemble of 73 REWs. Because of the fact that the model has been run for a long warm-up period the various internal state variables and fluxes have reached equilibrium. Water table positions, average saturation values and saturated area fractions have stabilized around their annual expected values, $E[y^s]$, $E[s^u]$ and $E[\omega^o]$, respectively. The same can be said about the various REW-internal and inter-REW mass fluxes. These are converted into water depths through division by the REW area.

[40] Figure 7c shows the expected value of the net mantle flux $E[\sum e^m]$ entering/exiting each REW laterally versus the sum of all remaining vertical mass fluxes for the saturated zone, namely the net groundwater recharge $E[e^{us}]$, the groundwater-river exchange $E[e^{rs}]$ and the seepage outflow $E[e^{os}]$. The lateral groundwater fluxes are non-measurable and thus a preliminary verification is carried out by looking at the overall water balance characteristics. We clearly see that part of the REWs are receivers of groundwater from neighboring REWs (positive flux) with a higher piezometric head, while other are donors losing water toward their neighbors (negative flux). The mean annual lateral groundwater exchange can reach up to 400 mm/year. The dots follow more or less a straight line, which is explained by the fact that the yearly average vertical groundwater input versus lateral exchange has essentially stabilized around an equilibrium, while a minor number of REWs are not at equilibrium and either loose on average more water laterally than they receive through vertical exchange, or vice versa. The REWs that loose water laterally are situated at the higher-lying southern boundary of the catchment (see Figures 5 and 6), while the receivers are situated at the center of the watershed. The leakage on the northern boundary causes the REWs located there (i.e., REWs 1, 73, 69, 52, 12, 13, 25, 26, 27, 39) to attract mass from more southern REWs with higher piezometric head levels and transfer mass across the flux boundary on the northern watershed edge.

[41] Figure 7d shows the net mean annual infiltration flux $E[e^{u\ top}]$ entering the unsaturated zone (precipitation minus evaporation) versus the net water table recharge $E[e^{us}]$ (percolation/capillary rise) on the water table. Also in this case the dots follow essentially a straight line, which

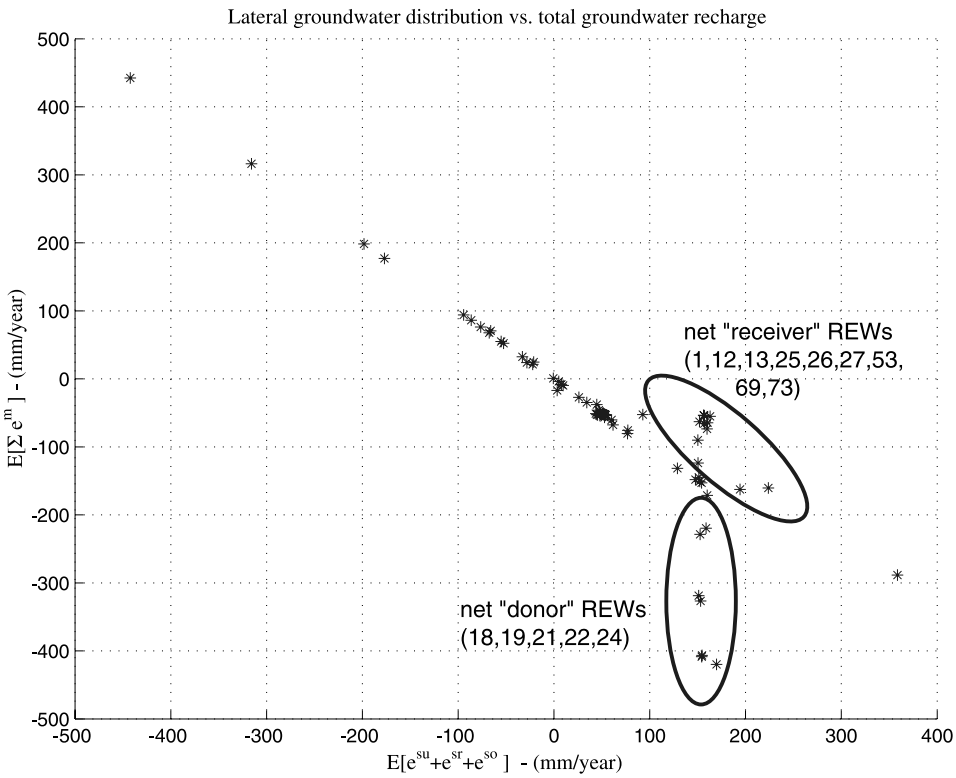

Figure 7c. Net lateral groundwater distribution in the saturated zone versus groundwater recharge.

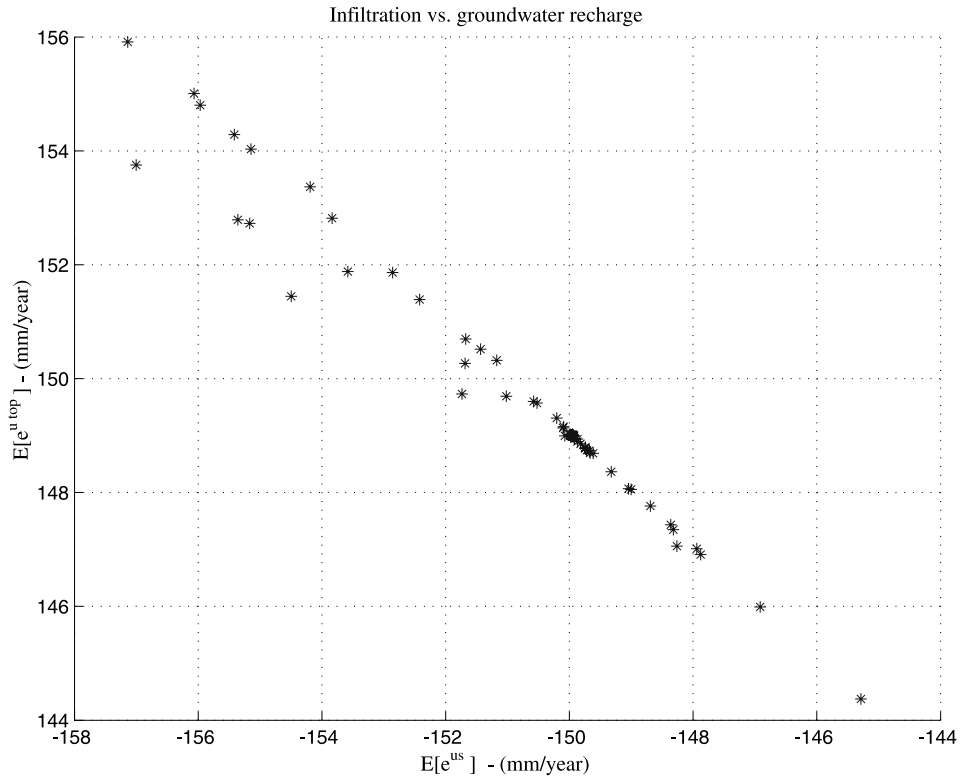

Figure 7d. Infiltration versus groundwater recharge.

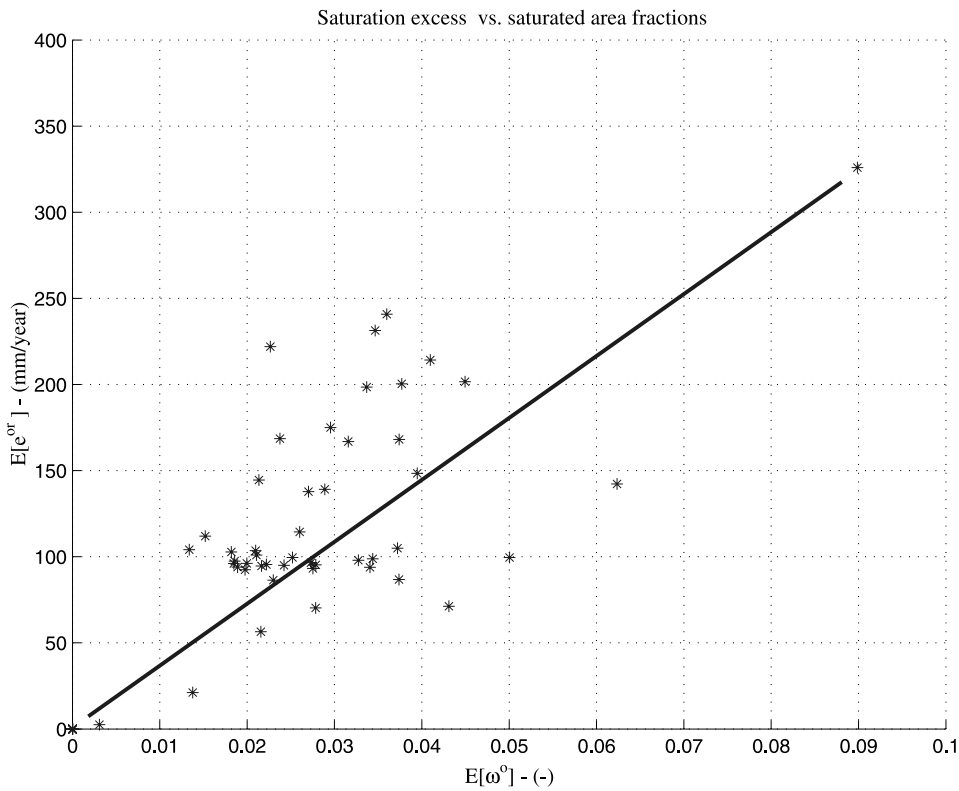

Figure 7e. Saturation excess versus saturated area fraction.

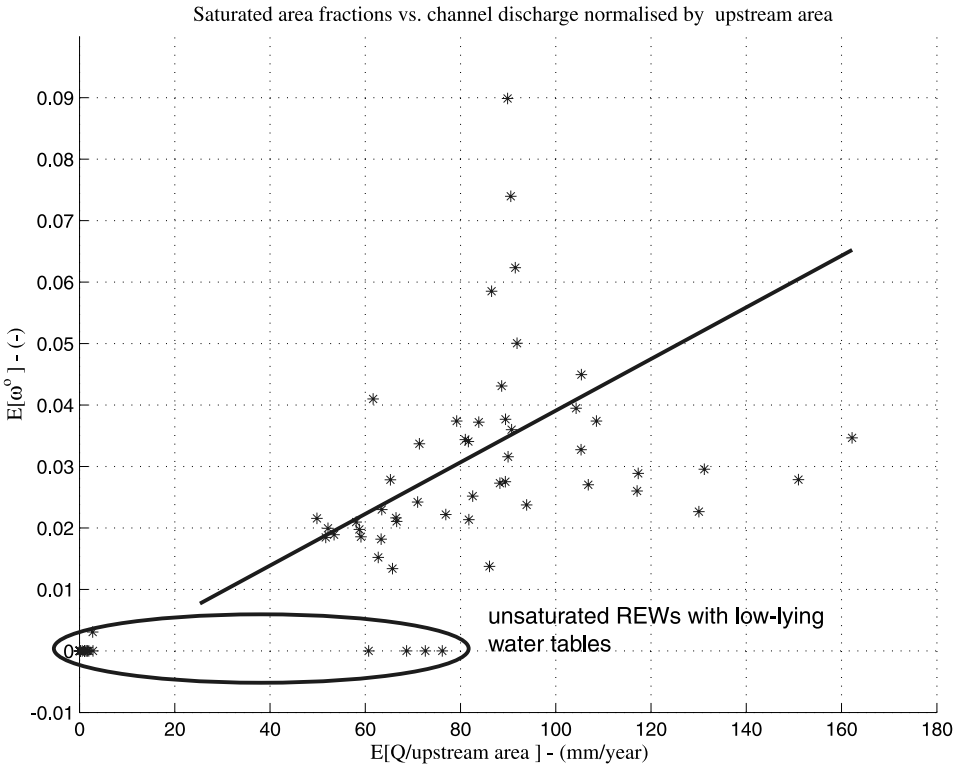

Figure 7f. Saturated area fractions versus channel discharge normalized by upstream area.

highlights that the average moisture content $E[s^u]$ in the unsaturated zone has reached equilibrium, with equal amounts of water entering and leaving the zone over a year on average. The net volume of water infiltrating the unsaturated zone is transferred directly toward the water table without any storage in the soil column. On average the net infiltration and water table recharge fluxes are situated in a narrow band between 145 and 158 mm/year for all REWs, which compares to the estimated recharge (equivalent to groundwater loss under steady conditions) indicated in equation (12) by adding the last two terms on the right-hand side.

[42] In Figure 7e we show the mean lateral inflow $E[e^{or}]$ (or saturation excess flow) generated by seepage and direct precipitation onto the saturated areas (reduced by the potential evaporation depth) versus the mean saturated REW area fractions $E[\omega^o]$. We note that the saturated area fractions range between 0% up to 10% of REW areas at the most. The saturation excess $E[e^{or}]$ contributes about 100 mm/year on average to runoff and reaches up to 250 mm/year for the REWs situated in the low part of the catchment with high-lying water tables. We observe a correlation between $E[e^{or}]$ and $E[\omega^o]$ as indicated by the solid black line. The saturation excess flow contributes fundamentally to sustaining the discharge in the stream network and constitutes a more important contribution to the base flow than the river-groundwater exchange $E[e^{rs}]$, which reaches on average 10 mm/year in the simulations. The presence of saturated areas contributes to the formation of the hydrograph peaks (by exfiltration and due to direct precipitation onto the saturated areas), that are generally underestimated in the present simulations. The expansion of the saturated areas also reflects the topographic features of the REW, as those with steeper surface slopes saturate to a lesser extend than flat REWs, where small groundwater fluctuations translate into larger saturated surface portions. Further work is however needed by testing nonlinear relationships $\omega^o = \omega^o(y^s)$ (see also section 3.3.4) between water table position and saturated area fraction and by including an additional zone for rapid subsurface flow to improve the peak discharge representation. We also observe that the saturated area extensions calculated here are not verified in the study site. However, the development of techniques that allow mapping of ω^o by e.g., remote sensing techniques could definitely add value to model validation and calibration.

[43] Figure 7f reports the relation between the saturated areas fractions and the channel outflow discharge for each REW normalized by the upstream catchment area. Also in this case we note a correlation between the discharge and the saturated area fraction. We also note that the maximum mean annual specific discharge for the outlet REW (REW 1) is 160 mm/year that is fairly close to the average stream discharge of 145 mm value estimated in equation (12) for the period 1975–1999. A series of REWs exhibit zero saturated area fractions $E[\omega^o]$ all year round. These are generally higher lying and the water table rarely reaches the land surface. In REWs with nonzero outflow and zero saturated area fraction the discharge is thus either due to inflow from upstream REWs or to base flow e^{rs} from the aquifer to the channel bed.

[44] Figure 7g compares the modeled water table responses for selected REWs with measured piezometric levels for the four piezometric wells F06, F29, ORTH022 and WAL66 indicated in Figure 6. The period 1987–1992 has been chosen because of availability of a complete set of piezometer data for that period. Generally the water table

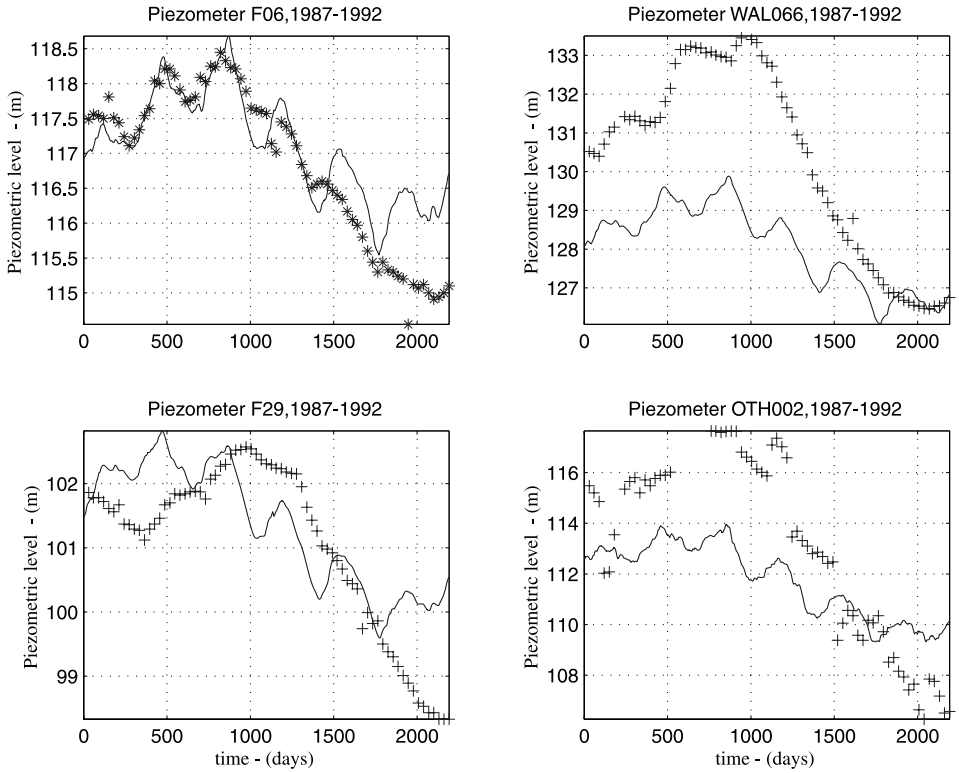

Figure 7g. Water table positions compared with measured piezometric heads for selected REWs during the simulation period 1987–1992.

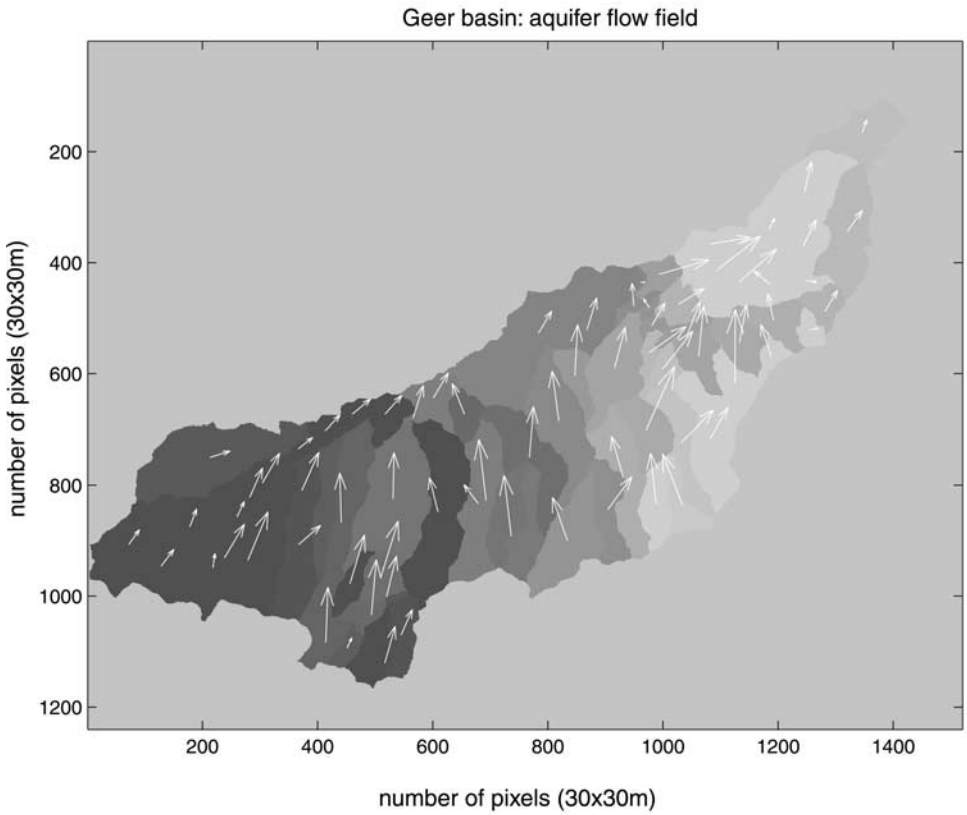

Figure 7h. Vector field representing the calculated horizontal velocities in the aquifer. See color version of this figure in the HTML.

fluctuations measured at the wells compare well with the average fluctuations simulated for REWs 39 (F06), 48 (F029), 49 (WAL66), and 51 (ORTH022), respectively. We note however that the REW approach calculates average water levels for an entire REW that can only be compared in particular situations with the measured piezometric levels (that represent *de facto* point values). Notably the Hesbaye aquifer is heavily exploited through pumping and two drainage galleries, which influence the shape of the water table locally. Reproducing its features accurately requires the use of a high-resolution 3-D aquifer model like the Finite Element solver described by *Dassargues et al.* [1988]. It is not the aim of the REW aquifer modeling approach to accurately represent localized phenomena, but rather to reproduce hydrological phenomena at the REW-averaged scale.

[45] Figure 7h gives a view of the 2-D horizontal flow field in the aquifer. The vectors are positioned at the respective centroid of each REW and indicate magnitude and direction of the velocity calculated from the momentum equation for the saturated zone in Table 4. The flow field is directed from the southern toward the northern permeable boundary, following the calculated hydraulic head distribution. We note that these results correspond with the calculations carried out by *Dassargues et al.* [1988]. Their piezometric head contours and aquifer flow field vectors (see Figure 10 in their paper) exhibit comparable directions and magnitude as those calculated with the REW saturated zone model, which is based on more simplistic assumptions on the hydraulic properties and flow dynamics of the subsurface.

[46] We conclude that the simulation results are promising, but still preliminary. The model is not yet calibrated or optimized in any way, the parameters used for the simulations have essentially been applied from point-scale values found in the literature to simulations at the REW scale. Moreover no spatial variability of the parameters has as yet been contemplated and the representation of the unsaturated zone by means of REW-scale flux formulations is still subject to ongoing research. To be able to draw more common and general conclusions about its performance, additional simulations for different catchments at various sizes and geographical locations are currently under way. The model parameter sensitivity analysis and alternative flux closure schemes are matter of ongoing research.

5. Conclusions

[47] An integrated simulation of a watershed system with the REW approach has been presented. The model results are still preliminary and some evident model errors are attributable to the chosen schematization, suboptimal parameter values, the spatial resolution and simplified flux representations. The REW concept had been introduced as an alternative modeling approach with different characteristics from the *Freeze and Harlan* [1969] blueprint or lumped conceptual models. The principal difference is due to the fact that the balance equations are used in an integral control volume type formulation. The principal effort in representing a system satisfactorily consists in parameterizing REW-scale mass fluxes and forces.

[48] Point-scale continuum approaches [e.g., *Freeze and Harlan*, 1969] offer the possibility to describe physical processes and variables in a distributed fashion, but remain computationally intensive and do not provide a consistent framework to accommodate gracefully the wide range of spatial and temporal scales. Modeling elements are assembled following numerical discretization grids that are adapted to computational schemes and needs, and not shaped after the morphology of the landscape. Conceptual lumped models on the other hand, while computationally efficient and robust, simplify the description of a hydrological system such that it is often no longer possible to identify spatially distributed and hydrologically interpretable dynamic variables or flow processes, as potentially required by the model end user community.

[49] The REW approach on the other hand preserves, in a somewhat simplified and integrated fashion, important hydrological interaction terms and descriptors such as piezometric heads, velocities and saturated area fractions, while using megascale balance laws as governing equations. The megascale representation yields a flux-based description of the system via mass and momentum interactions on its boundaries, in contrast to continuum formulations that contemplate internal gradients. The megascopic formulation, stated in terms of suitably chosen control volumes allows to circumvent structurally scale inconsistencies and reduces the problem to the specification of megascopic fluxes and forces between control volume interfaces. The present application aims at showing how an integrated watershed system, including vadose zone flow, groundwater, overland and channel flow is modeled in terms of REW-scale flux formulations and global balance laws. It is recognized that the proposed flux formulations are in part still preliminary and incomplete, and that further work is needed to improve these. The improvements should be based on additional theoretical work, such as approximated analytical solutions of unsaturated zone water fluxes, or on the exploitation of research results from innovative observation and measurement techniques. We observe, however that any flux representation requires ultimately recurrence to parameter values that need to be either measured or identified by calibration or other means such as inverse procedures. Parameterization will require the reversion to effective values, and thus give raise to equifinality of parameter sets discussed in the literature [e.g., *Beven*, 2001]. The interpretability of the fluxes in terms of physical principles in the REW approach can however guide within reasons the choice of the parameter values, in contrast to lumped conceptual models. Moreover, for given hydrological situations where internal system variability has a nonnegligible impact on its hydrological response characteristics, the proposed approach may result less efficient than continuum-type models. A choice on the most suitable formulation has to be made on a case-by-case basis.

[50] For future research the REW approach provides a modeling platform that can be utilized to experiment and test improved schematization of the hydrological fluxes [*Beven*, 2000, 2002]. If higher spatial resolutions are to be achieved, smaller elements that are selected based on land cover pattern or soil type, can be defined within the REW and global balance laws applied in terms of the same principles shown so far. The implementation of the

approach, as presented here, constitutes a more general modeling platform suited for adding additional features such as hydrologically driven transport of solutes or sediment. The present work provides thus an alternative framework for hydrological applications of various type with potential use for a wide ranging end user community from scientific hydrologists to water managers and planners.

[51] **Acknowledgments.** We would like to thank the Hydrogeology team of the University of Liège (Belgium) and especially S. Brouyère and A. Dassargues for providing the basic data about the geological and hydrogeological conditions in the Geer basin. We would also like to thank the Royal Meteorological Observatory (KMI) in Brussels and E. Roulin for having provided the digital elevation maps and the hydrometeorological data. A large party of the work has been carried out within the project DAUFIN, sponsored by the European Commission within the Framework Programme V under contract number EVK1-CT1999-00022. Last, but not least, our thanks go also to K. Beven for his support and encouraging discussions during the EFFS (European Commission contract number EVK1-CT1999-00011) project meetings and to two anonymous referees, who have contributed to improving the manuscript.

References

Abbott, M. B., J. C. Bathurst, J. A. Cunge, P. E. O'Connell, and J. Rasmussen (1986a), An introduction to the European Hydrological System–Système Hydrologique Européen, SHE, 1. History and philosophy of a physically based, distributed modeling system, *J. Hydrol.*, *87*, 45–59.

Abbott, M. B., J. C. Bathurst, J. A. Cunge, P. E. O'Connell, and J. Rasmussen (1986b), An introduction to the European Hydrological System–Système Hydrologique Européen, SHE, 2. Structure of a physically-based, distributed modeling system, *J. Hydrol.*, *87*, 61–77.

Bergström, S. (1995), The HBV model, in *Computer Models of Watershed Hydrology*, edited by V. P. Singh (Ed.), pp. 443–476, Water Resour. Publ., Highlands Ranch, Colo.

Beven, K. (1989), Changing ideas in hydrology—The case of physically-based models, *J. Hydrol.*, *105*, 157–172.

Beven, K. J. (1996), A discussion on distributed modeling, in *Distributed Hydrological Modelling*, edited by C. J. Reefsgard and M. B. Abbott, pp. 255–278, Springer, New York.

Beven, K. J. (2000), Uniqueness of place and process representations in hydrological modeling, *Hydrol. Earth Syst. Sci.*, *4*(2), 203–213.

Beven, K. J. (2001), How far can we go in distributed hydrological modeling?, *Hydrol. Earth Syst. Sci.*, *5*(1), 1–12.

Beven, K. J. (2002), Towards an alternative blueprint for a physically-based digitally simulated hydrologic response modeling system, *Hydrol. Processes*, *16*, 189–206, doi:10.1002/hyp.343.

Beven, K. J., and M. J. Kirkby (1979), A physically based, variable contributing area model of basin hydrology, *Hydrol. Sci. Bull.*, *24*(1), 43–69.

Bronstert, A. (1999), Capabilities and limitations of detailed hillslope hydrological modeling, *Hydrol. Processes*, *13*, 21–48.

Brooks, R. H., and C. T. Corey (1964), Hydraulic properties of porous media, *Hydrol. Pap. 3*, Colo. State Univ., Fort Collins.

Brouyère, S., G. Carabin, and A. Dasargues (2004), Climate change impacts on groundwater reserves: Modelled deficits in a chalky aquifer, Geer basin, Belgium, *Hydrogeol. J.*, *12*(2), 123–134, doi:10.1007/s10040-003-0293-1.

Calver, A., and W. L. Wood (1995), The Institute of Hydrology distributed model, in *Computer Models of Watershed Hydrology*, edited by V. P. Singh, pp. 595–626, Water Resour. Publ., Highlands Ranch, Colo.

Cash, J. R., and A. H. Karp (1990), A variable order Runge-Kutta method for initial value problems with rapidly varying right hand sides, *ACM Trans. Math. Software*, *16*(3), 201–222.

Crawford, N. H., and R. K. Linsley (1966), Digital simulation in hydrology, Stanford Watershed Model IV, *Tech. Rep. 39*, Dep. of Civ. Eng., Stanford Univ., Stanford, Calif.

Cross, H. (1936), Analysis of Flow in Networks of Conduits or Conductors, *Bull. 286*, Univ. of Ill., Urbana.

Dassargues, A., and A. Monjoie (1993), Chalk as an aquifer in Belgium, in *Hydrogeology of the Chalk of North-West Europe*, pp. 153–169, Oxford Univ. Press, New York.

Dassargues, A., J. P. Radu, and R. Charlier (1988), Finite elements modeling of a large water table aquifer in transient conditions, *Adv. Water Resour.*, *11*(2), 58–66.

Doucet, A., N. de Freitas, and N. Gordon (2001), An introduction to sequential Monte Carlo methods, in *Sequential Monte Carlo Methods in Practice*, edited by A. Doucet, N. de Freitas, and N. Gordon, pp. 3–14, Springer, New York.

Duan, Q., V. K. Gupta, and S. Sorooshian (1993), A shuffled complex evolution approach for effective and efficient global minimization, *J. Optim. Theory Appl.*, *76*(3), 501–521.

Duffy, C. J. (1996), A two-state integral-balance model for soil moisture and groundwater dynamics in complex terrain, *Water Resour. Res.*, *32*(7), 2421–2434.

Freeze, R. A., and R. L. Harlan (1969), Blueprint for a physically-based, digitally-simulated hydrologic response model, *J. Hydrol.*, *9*, 237–258.

Gray, W. G., A. Leijnse, R. L. Kolar, and A. C. Blain (1993), *Mathematical Tools for Changing Spatial Scales in the Analysis of Physical Systems*, CRC Press, Boca Raton, Fla.

Grayson, R. B., I. D. Moore, and T. A. McMahon (1992), Physically based hydrological modeling: 2. Is the concept realistic?, *Water Resour. Res.*, *26*(10), 2659–2666.

Haverkamp, R., J. Y. Parlange, J. L. Starr, G. Shmitz, and C. Fuentes (1990), Infiltration under ponded conditions: 3. A predictive equation based on physical parameters, *Soil Sci.*, *149*(5), 242–300.

Leavesley, G. H., R. W. Lichty, B. M. Troutman, and L. G. Saindon (1983), Precipitation-runoff modeling system: User's manual, *U.S. Geol. Surv. Water Resour. Invest. Rep., 83-4238*, 207 pp.

Leopold, L. B., and T. Maddock (1953), The hydraulic gemotry of stream channels and some physiographic implications, *U.S. Geol. Surv. Prof. Pap.*, *253*, 9–16.

Naden, P., P. Broadhurst, N. Tauveron, and A. Walker (1999), River routing at the continental scale; use of globally available data and an a priori method of parameter estimation, *Hydrol. Earth Syst. Sci.*, *3*, 109–124.

O'Connell, P. E., and E. Todini (1996), Modeling of rainfall, flow and mass transport in hydrological systems: An overview, *J. Hydrol.*, *175*, 3–16.

Press, W. H., S. A. Teukolsky, W. T. Vetterling, and B. P. Flannery (1994), *Numerical Recipies in C*, Cambridge Univ. Press, New York.

Refsgaard, J. C., and B. Storm (1996), Comment on "A discussion on distributed modelling" by K.J. Beven, in *Distributed Hydrological Modeling*, edited by C. J. Reefsgard and M. B. Abbott, pp. 279–287, Springer, New York.

Reggiani, P., M. Sivapalan, and S. M. Hassanizadeh (1998), A unifying framework of watershed thermodynamics: 1 Balance equations for mass, momentum, energy and entropy and the second law of thermodynamics, *Adv. Water Resour.*, *22*(4), 367–398.

Reggiani, P., M. Sivapalan, S. M. Hassanizadeh, and W. G. Gray (1999), A unifying framework of watershed thermodynamics: 2 Constitutive relationships, *Adv. Water Resour.*, *23*(1), 15–39.

Reggiani, P., M. Sivapalan, and S. M. Hassanizadeh (2000), Conservation equations governing hillslope responses, *Water Resour. Res.*, *38*(7), 1845–1863.

Reggiani, P., M. Sivapalan, S. M. Hassanizadeh, and W. G. Gray (2001), Balance equations for mass and momentum in a channel network: Theoretical derivation and computational experiments, *Proc. R. Soc. London, Ser. A*, *457*, 157–189.

Snell, J. D., and M. Sivapalan (1995), Application of the meta-channel concept: Construction of the meta-channel hydraulic geometry for a natural catchment, in *Scale Issues in Hydrological Modeling*, edited by J. D. Kalma and M. Sivapalan, pp. 241–261, John Wiley, Hoboken, N. J.

Soil Conservation Service (1972), *National Engineering Handbook, Section 4, Hydology*, U.S. Dep. of Agric., Washington D. C.

Tarboton, D. G. (1997), A new method for the determination of flow directions and contributing areas in grid digital elevation models, *Water Resour. Res.*, *33*(2), 309–319.

Van der Kwaak, J. E., and K. Loague (2001), Hydrologic-response simulations for the R-5 catchment with a comprehensive physics-based model, *Water Resour. Res.*, *37*(5), 999–1013.

Viney, N. R., and M. Sivapalan (1999), A conceptual model of sediment transport: Application to the Avon River Basin in Western Australia, *Hydrol. Processes*, *13*, 727–743.

P. Reggiani, Foundation Delft Hydraulics, P.O. Box 177, 2600MH, Delft, Netherlands. (paolo.reggiani@wldelft.nl)

T. H. M. Rientjes, International Institute for Geo-Information Science and Earth Observation, P.O. Box 6, 7500AA, Enschede, Netherlands. (rientjes@itc.nl)